Received: 24 March 2023 | Revised: 11 April 2023 | Accepted: 12 April 2023

DOI: 10.1002/ardp.202300174

FULL PAPER

ARCH PHARM DPhG
Archiv der Pharmazie

Selective noncovalent proteasome inhibiting activity of trifluoromethyl-containing *gem*-quaternary aziridines

Laura Ielo[1] | Vincenzo Patamia[2] | Andrea Citarella[3] | Tanja Schirmeister[4] | Claudio Stagno[5] | Antonio Rescifina[2] | Nicola Micale[5] | Vittorio Pace[1,6]

[1]Department of Chemistry, University of Turin, Torino, Italy

[2]Department of Drug and Health Sciences, University of Catania, Catania, Italy

[3]Department of Chemistry, University of Milan, Milano, Italy

[4]Department of Medicinal Chemistry, Institute of Pharmaceutical and Biomedical Sciences, Johannes Gutenberg University, Mainz, Germany

[5]Department of Chemical, Biological, Pharmaceutical and Environmental Sciences, University of Messina, Messina, Italy

[6]Department of Pharmaceutical Sciences, Division of Pharmaceutical Chemistry, University of Vienna, Vienna, Austria

Correspondence
Vittorio Pace and Laura Ielo, Department of Chemistry, University of Turin, Via P. Giuria 7, 10125 Torino, Italy.
Email: vittorio.pace@unito.it and laura.ielo@unito.it

Funding information
University of Turin, University of Vienna and University of Mainz

Abstract

The ubiquitin-proteasome pathway (UPP) represents the principal proteolytic apparatus in the cytosol and nucleus of all eukaryotic cells. Nowadays, proteasome inhibitors (PIs) are well-known as anticancer agents. However, although three of them have been approved by the US Food and Drug Administration (FDA) for treating multiple myeloma and mantel cell lymphoma, they present several side effects and develop resistance. For these reasons, the development of new PIs with better pharmacological characteristics is needed. Recently, noncovalent inhibitors have gained much attention since they are less toxic as compared with covalent ones, providing an alternative mechanism for solid tumors. Herein, we describe a new class of bis-homologated chloromethyl(trifluoromethyl)aziridines as selective noncovalent PIs. In silico and in vitro studies were conducted to elucidate the mechanism of action of such compounds. Human gastrointestinal absorption (HIA) and blood–brain barrier (BBB) penetration were also considered together with absorption, distribution, metabolism, and excretion (ADMET) predictions.

KEYWORDS
aziridines, homologation, *in silico* assays, in vitro assays, noncovalent proteasome inhibitors

1 | INTRODUCTION

The ubiquitin-proteasome pathway (UPP) represents the principal proteolytic apparatus in the cytosol and nucleus of all eukaryotic cells. It is responsible for preserving intracellular protein homeostasis in physiological and adaptive stress conditions.[1,2] The degradation of the targeted proteins by UPP is a cyclic pathway characterized by the initial ubiquitination of damaged or abnormal proteins.[3–5] Indeed, these polyubiquitinated proteins are then degraded via the 26S proteasome system. The 26S eukaryotic proteasome is a multifunctional macromolecule featured by a 20S core particle (CP), the proteolytically active part, and two 19S outer regulatory particles (RPs). Four heptameric rings stacked in an α7β7β7α7 arrangement constitute the CP. Among the β1–7 proteolytic active sites of the two inner β-rings, β1, β2, and β5 subunits are the proteolytic ones with different substrate specificities.[6–8] β5 subunits display "chymotrypsin-like" (ChT-L) activity and are mostly involved in protein degradation. For this reason, they constitute the main targets for developing anticancer agents.[9] β2 and β1 subunits instead are considered as cotargets. β2 subunits possess "trypsin-like" (T-L) activity, whereas β1 are referred to as subunits with

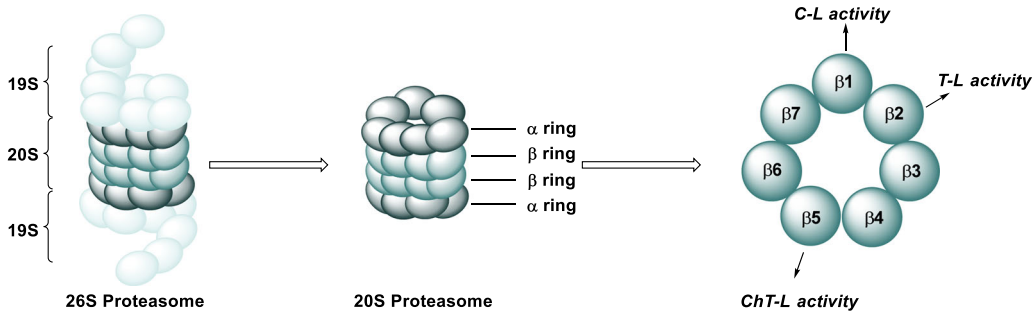

FIGURE 1 Schematic structure of the 26S proteasome.

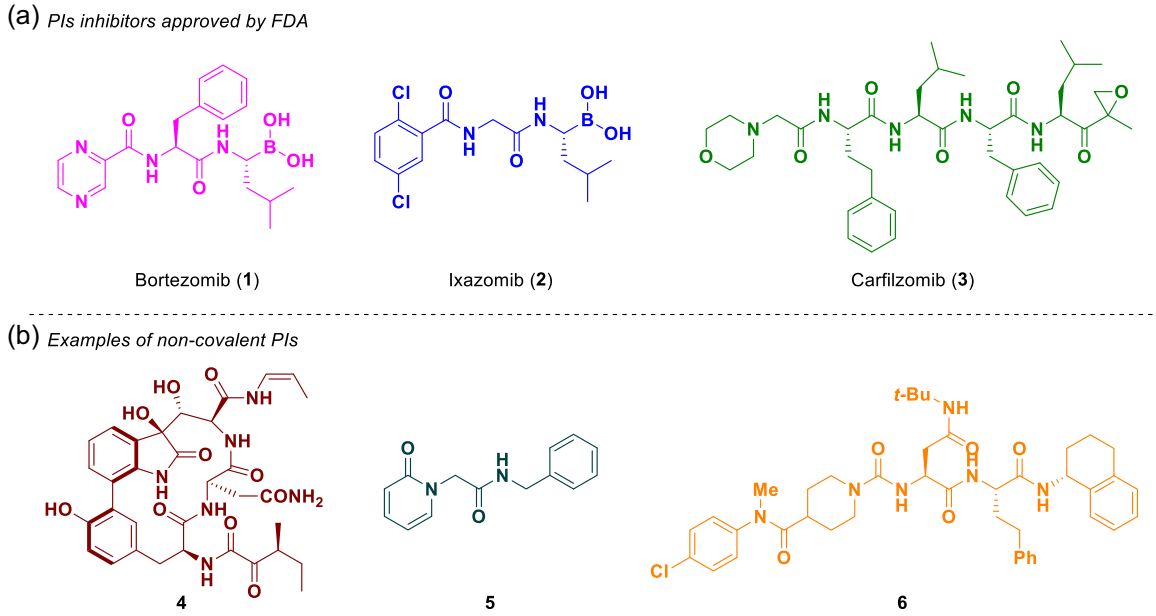

FIGURE 2 Proteasome inhibitors (PIs) approved by Food and Drug Administration (FDA) (a). Examples of noncovalent PIs (b).

"post-glutamate peptide hydrolase" (PGPH) or "caspase-like" (C-L) activity (Figure 1).[10,11] All three catalytic subunits contain an *N*-terminal residue represented by Thr1. The hydroxyl group of Thr1 carries out the nucleophilic attack to the peptide bond, playing a central role in the formation of the tetrahedral intermediate of the proteolytic mechanism. A water molecule then completes the degradation of the peptide, performing the hydrolysis with the release of the catalytic Thr1.[12,13]

To date, three kinds of proteasomes have been investigated: the constitutive proteasome (cCP),[14–16] which is the most widely distributed in cells, the immunoproteasome (iCP),[17,18] and the thymoproteasome (tCP),[19] which are responsible for the antigen presentation and the positive selection of $CD8^+$ T cells, respectively.

The employment of proteasome inhibitors (PIs) as anticancer agents is well-established nowadays.[20,21] Indeed, three PIs, bortezomib (**1**),[22] ixazomib (**2**), and carfilzomib (**3**) have been approved by the US Food and Drug Administration (FDA) for the treatment of multiple myeloma and mantel cell lymphoma (Figure 2a).[23] The clinically used PIs, as well as the major part of the inhibitors reported in the literature, are covalent. They are characterized by different electrophilic warheads able to bind the hydroxyl group of the N-terminal threonine residue of the 20S catalytic β5-subunit.[24] Even if they show great efficiency in anticancer therapy, the covalent mode of action leads to severe side effects[25,26] and limited activities in solid tumors.[27] Therefore, their clinical use has been limited due to a lack of specificity and excessive reactivity and instability. On the other hand, promising diverse noncovalent inhibitors (e.g., **4**, **5**, and **6**) have been identified, showing reduced toxicity and providing a different mechanism for solid tumors due to the rapid binding and dissociation kinetics of the noncovalent interactions (Figure 2b).[14]

Considering the results achieved so far regarding the development of noncovalent PIs[28–31] and in agreement with preliminary docking studies, the inhibitory activity of a set of bis-homologated

chloromethyl(trifluoromethyl)aziridines (CMTMAs) was evaluated toward this anticancer target.[32]

2 | RESULTS AND DISCUSSION

2.1 | Pharmacology/Biology

The preparation of the targeted CMTMAs was levered on the homologation logic of imine surrogates with nucleophilic lithium carbenoids[33,34] previously reported.[32] Compounds **8**–**19** (Figure 3) were then evaluated in vitro against human 20S proteasome, and the results are reported in Table 1.

The ChT-L activity (β5 subunit) against human 20S proteasome was assessed for all CMTMAs (**8**–**19**) at a concentration of 20 μM using dimethyl sulfoxide (DMSO) as a negative control.[36] The three most active CMTMAs (i.e., **10**, **12**, and **19**) showed inhibitory activity of 67%, 73%, and 80%, respectively, suggesting that bulky hydrophobic groups connected to the aziridine nitrogen are favored for efficacious binding to the target. Furthermore, as in **12** and **19**, substituents in *meta*-position were well tolerated, as well as basic substituents, such as morpholinyl (as in **10**) and pyrrolidinyl (as in **19**). Thus, continuous assays were carried out for **10**, **12**, and **19**, showing IC_{50} values of 12.1, 11.3, and 9.8 μM, respectively, and binding affinity values (K_i) in the low-micromolar range (Table 1).

Comparing the biological activity of the CMTMAs with the previously reported chloro(trifluoromethyl)aziridines (CTMAs),[29] a clear correlation of how the substituents influence the activity was not found. Even if the two series of compounds differ only for a methylene unit, a different percentage of inhibition was found for

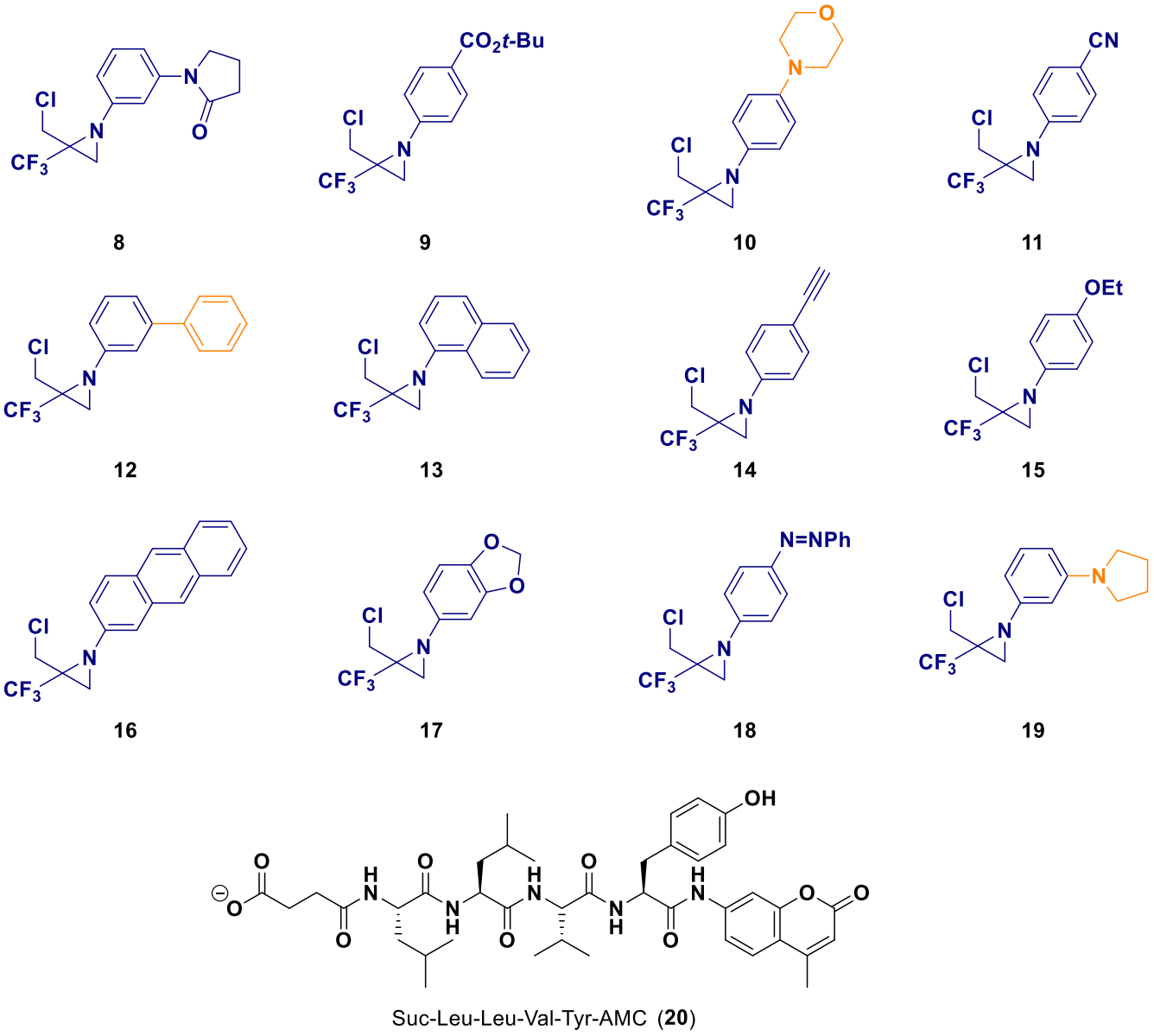

FIGURE 3 Chemical structures of compounds **8**–**19** and reference compound **20**.

TABLE 1 Docking scores and predicted K_i on proteasome subunit β5 of *Saccharomyces cerevisiae* (PDB ID: 4HRD) as well as inhibitory activities of compounds **8**–**19** compared with reference [20].

Compound	ΔG Vina	K_i calc. (μM)	ChT-L activity (% inhibition at 20 μM)[a]	IC_{50}/K_i (μM) ChT-L[b]
8	−8.70	0.42	23 ± 0.1	—
9	−7.19	5.33	<20	—
10	−8.18	1.00	67 ± 0.4	12.1 ± 0.2/1.4 ± 0.02
11	−7.64	2.49	<20	—
12	−8.66	0.45	73 ± 0.5	11.3 ± 0.6/1.3 ± 0.07
13	−7.94	1.50	<20	—
14	−7.64	2.49	38 ± 1.3	—
15	−6.91	8.56	<20	—
16	−8.14	1.07	25 ± 0.9	—
17	−7.76	2.04	<20	—
18	−8.42	0.67	36 ± 1.0	—
19	−7.15	5.71	80 ± 0.9	9.8 ± 0.7/1.1 ± 0.08
20	−8.75	0.38	—	K_i = 0.35[35]
Bortezomib[c]	—	—	100	0.085 ± 0.002/0.0098 ± 0.001[28]

[a]Screening assays on human 20S proteasome ChT-L activity (β5 subunits).

[b]Continuous assays on human 20S proteasome ChT-L activity (β5 subunits) with final inhibitor concentrations 0, 2.5, 5, 10, 20, 30, 40, and 50 μM performed for 30 min only for compounds that showed > 60% of inhibition in the screening test. IC_{50} values include standard deviation from two independent experiments performed in duplicate. K_i ± SD values have been calculated using the Cheng–Prusoff equation. The K_m values were determined in separate experiments: For ChT-L activity with Suc-Leu-Leu-Val-Tyr-AMC K_m = 13 μM.

[c]Values determined in the same experimental conditions of CMTMAs.

the derivatives embodied with an anthracenyl (**16**), pyrrolidinyl (**19**), diazophenyl (**18**), and morpholinyl (**10**) moieties. Indeed, for the CTMAs the best activity was observed for the anthracene- (IC_{50} = 13.6 μM) and diazophenyl- (IC_{50} = 14.1 μM) bearing compounds,[29] whereas for the CMTMAs the presence of a phenyl group in *ortho* position (**12**), a morpholinyl (**10**), and a pyrrolidinyl (**19**) functionalities led to the most active molecules. Neither the position nor the presence of electron-withdrawing or electron-donating groups clearly explained the variation of the activity. Despite the unclear correlation between the various substituents linked to the aziridine moiety, comparing the results obtained from the docking studies carried out in the previous work and this one, it appears that the interactions with the various residues of the receptor site are almost conserved, albeit with different portions of the molecules, for example, with residues Ala20, Ala27, Ser28, and Glu132. Each of these residues interacts with both the previous ligands and those reported in this work, albeit through interactions of a different nature.

Preliminary assays (i.e., screening at 20 μM) performed on various cysteine and serine proteases (i.e., human cathepsins B and L, and bovine pancreatic α-chymotrypsin) to assess off-target reactivity, as well as on proteasome β1 and β2 subunits, did not display any inhibitory activity (inhibition range 0%–5%), demonstrating a marked selectivity of compounds **8**–**19** against proteasome β5 subunits.

2.2 | Molecular modeling studies and absorption, distribution, metabolism, and excretion (ADMET) prediction

In silico studies were performed using AutoDock Vina implemented in the yet another scientific artificial reality application (YASARA) software. The docking studies were performed on all the protonation states of the compounds at pH 7.4, previously calculated using the Marvin software. The peptide Suc-Leu-Leu-Val-Tyr-AMC (**20**, Figure 3) was used as a reference proteasome substrate. The calculated inhibition constants are reported in Table 1 and, for the best-performing compounds, **10**, **12**, and **19**, agree well with the experimental ones.

Figure 4 shows the 3D and 2D poses of the three best compounds, **10**, **12**, and **19**. From the interactions dictated at the poses within the receptor pocket, it is evident that the aromatic ring of these compounds acts as the anchor portion; in fact, we note in all three compounds π–cation and π–anion interactions, in particular, compound **10** establishes these interactions with residues Glu132, Glu134, and Arg137, compound **12** with residues Asp126 and Arg137, and compound **19** with residue Arg137. The presence of other similar interactions, such as hydrophobic, π-alkyl, and with halogens, reflects the similar inhibitory activity of the three compounds toward the proteasome. For example, compounds

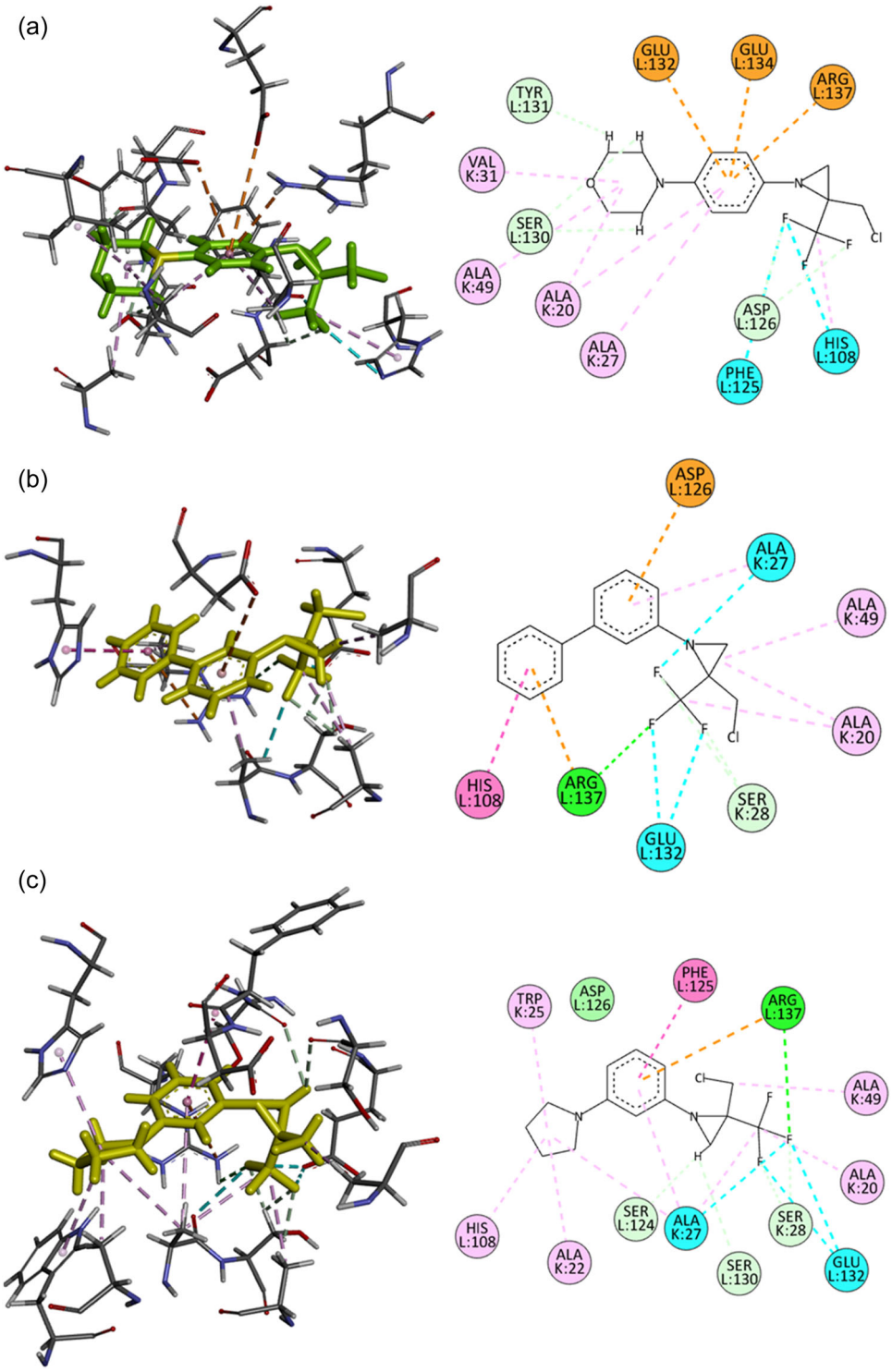

FIGURE 4 3D and 2D poses of compounds **10** (a), **12** (b), and **19** (c) within the receptor pocket.

12 and **19** (Figure 4b,c) establish the same interactions with the identical residues Ala20, Ala27, Ala49, Ser28, and Arg137.

To better study the formation and stability of the ligand@protein complex, 100 ns of molecular dynamics (MD) simulations for ligands **10**, **12**, and **19** were performed within the receptor pocket of the proteasome. From the graphs shown in Figure 5, analyzing the total energy and the root-mean-square deviation of the complexes, it is evident that all three ligands form a very stable complex within the receptor site; this is due to the dense network of interactions, previously commented on, that keeps the ligands anchored within the receptor pocket.

The in silico assessment has been expanded by evaluating pharmacokinetic profiles and possible adverse side effects for ligands **10**, **12**, and **19**. The ability to reach the target was assessed

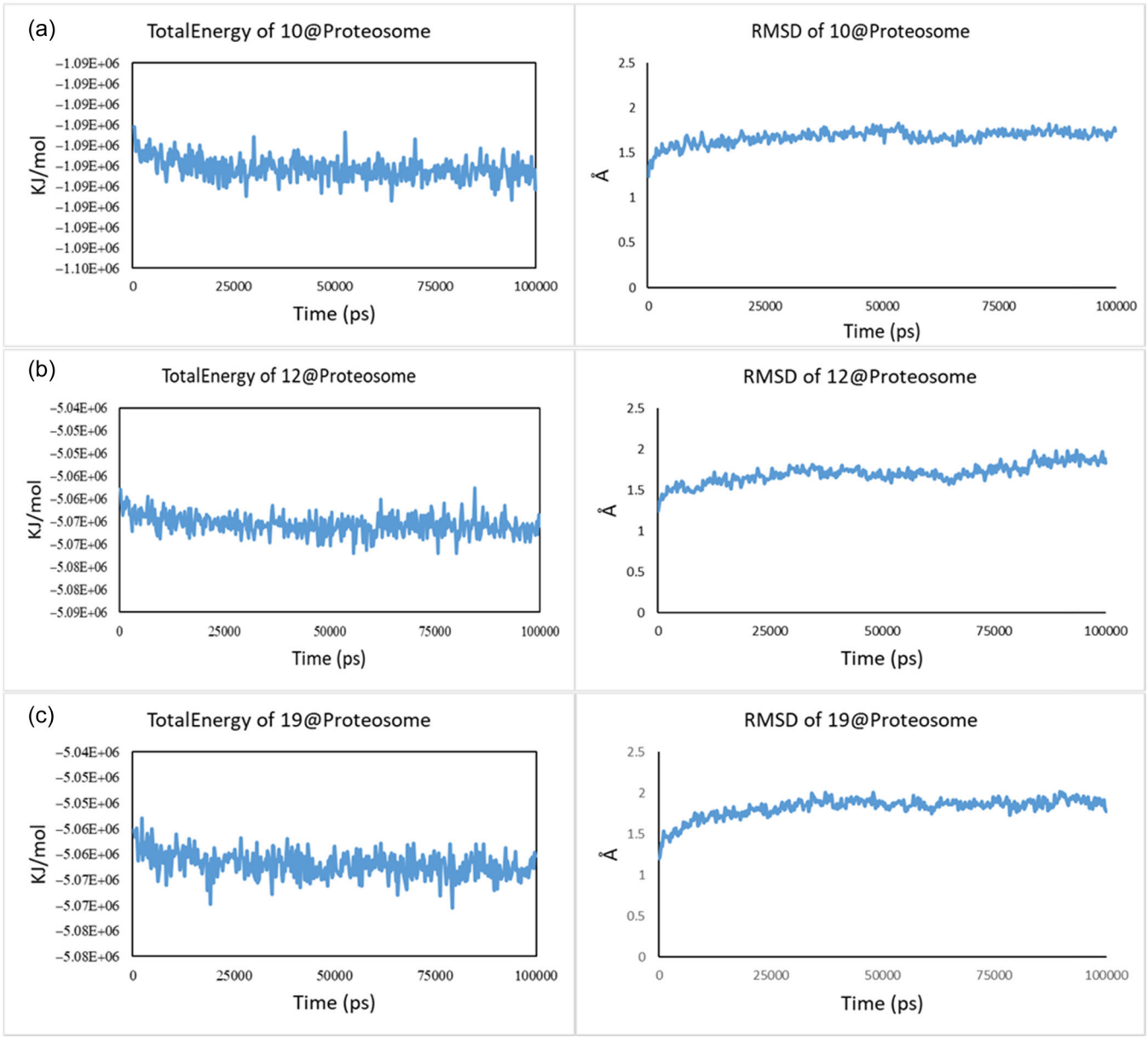

FIGURE 5 Total energy and RMSD of the ligand@protein complexes for compounds **10** (a), **12** (b), and **19** (c) within the proteasome. RMSD, root-mean-square deviation.

TABLE 2 GI absorption, drug-likeness, lead-likeness, bioavailability score, PAINS, and synthetic accessibility parameters of compounds **10**, **12**, and **19**.

Compound	GI absorption	Lipinski	Ghose	Veber	Egan	Muegge	Lead-likeness	Bioavailability score	PAINS alerts	Synthetic accessibility
10	High	0	0	0	0	0	0	0.55	1	2.76
12	Low	1	0	0	0	2	1	0.55	0	2.65
19	High	0	0	0	0	0	1	0.55	0	2.84

Abbreviation: GI, gastrointestinal; PAINS, pan-assay interference compounds.

using the SwissADME server (http://swissadme.ch), accessed on February 10, 2022), and the results are reported in Table 2. These evaluations show that compounds **10** and **19** simultaneously satisfy the drug-likeness rules of Lipinski,[37] Ghose,[38] Veber,[39] Egan,[40] and Muegge.[41] Notably, **12** and **19** showed no alerts on the outcome of the pan-assay interference compounds model of pan assay interference structures, designed to exclude small molecules that might show false positives in bioassays. In addition,

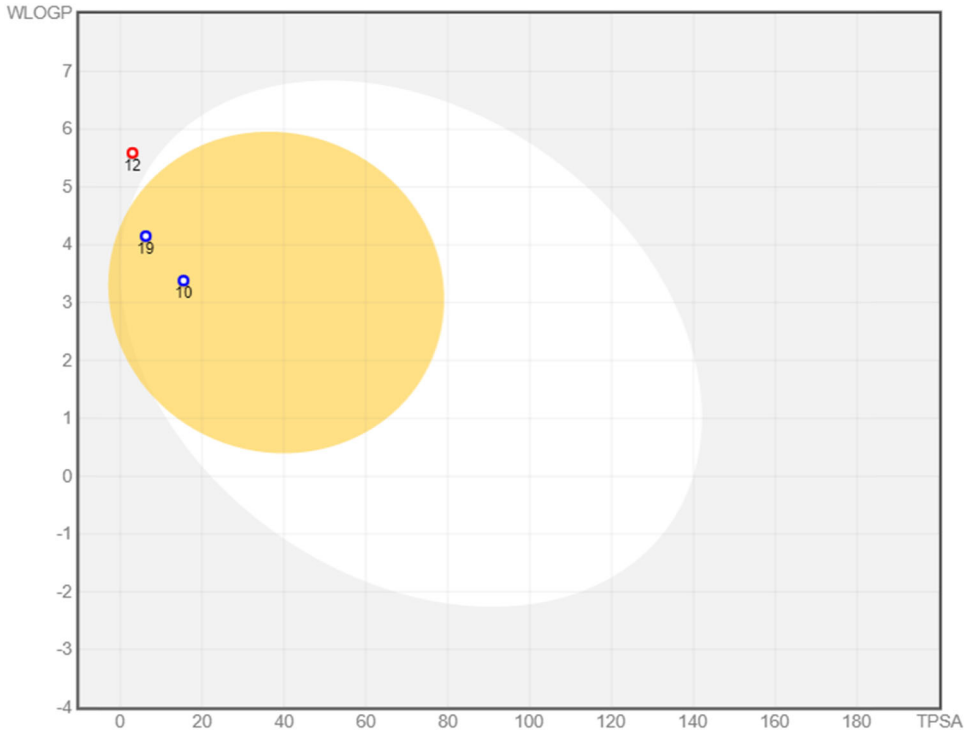

FIGURE 6 BOILED-Egg plot. Points located in the BOILED-Egg's yolk (yellow) represent the molecules predicted to passively permeate through the blood–brain barrier, whereas the ones in the egg white are relative to the molecules predicted to be passively absorbed by the gastrointestinal tract; the blue dots (**10** and **19**) indicate the molecules for which it was expected to be effluated from the CNS by the P-glycoprotein, whereas the red ones (**12**) point to the molecules predicted not to be effluated from the CNS by the P-glycoprotein. CNS, central nervous system.

all three compounds show a bioavailability score of 0.55 and excellent synthetic accessibility, the latter being critical to meeting the interests of pharmaceutical industries.

Human gastrointestinal absorption (HIA) and blood–brain barrier (BBB) penetration, related to absorption and distribution parameters, respectively, were graphically represented by the extended and revamped version of the Edan-Egg model, called Brain Or IntestinaL EstimateD (BOILED) predictive permeation model (BOILED-Egg).[42] Analyzing Figure 6, we note that compounds **10** and **19** passively cross the BBB, and both, with the help of P-glycoprotein, can be effluated from the central nervous system (CNS); on the other hand, molecule **12** is not passively absorbed from the gastrointestinal tract.

3 | CONCLUSION

In conclusion, the inhibitory activity toward the proteasome of a new class of aziridine derivatives has been reported. In silico studies predicted a noncovalent mechanism of action and promising "drug-like" features as anticancer agents. In vitro enzymatic assays revealed a selective inhibition over the β5 proteasome subunits. Moreover, preliminary studies were conducted on several cysteine and serine proteases (i.e., human cathepsins B and L, and bovine pancreatic α-chymotrypsin) to assess off-target reactivity and did not show any inhibitory activity.

4 | EXPERIMENTAL

4.1 | Chemistry

4.1.1 | General

Melting points were determined on a Reichert–Kofler hot-stage microscope and uncorrected. Mass spectra were obtained on a Shimadzu QP 1000 instrument (EI, 70 eV) and a Bruker maXis 4 G instrument (ESI-TOF, HRMS). ^{1}H, ^{13}C, ^{19}F, and ^{15}N nuclear magnetic resonance (NMR) spectra were recorded using a Bruker Avance III 400 spectrometer (400 MHz for ^{1}H, 100 MHz for ^{13}C, 377 MHz for ^{19}F, 40 MHz for ^{15}N) and a Bruker DRX spectrometer (200 MHz for ^{1}H, 50 MHz for ^{13}C) at 297 K. The center of the solvent signal was used as an internal standard which was related to tetramethylsilane with δ 7.26 ppm (^{1}H in $CDCl_3$), δ 77.00 ppm (^{13}C in $CDCl_3$). ^{15}N NMR spectra were referenced against external nitromethane (0.0 ppm), and ^{19}F NMR spectra by absolute referencing via ∈ ratio. Spin–spin coupling constants (*J*) are given in Hertz. In nearly all cases, complete and unambiguous assignment of all resonances was performed by applying standard NMR techniques, such as attached proton test, heteronuclear single quantum coherence, heteronuclear multiple bond correlation, correlation spectroscopy, and nuclear overhauser effect experiments.

Tetrahydrofuran (THF) was distilled over Na/benzophenone. Chemicals were purchased from Sigma-Aldrich, Acros, Alfa Aesar,

Fluorochem, and TCI Europe, otherwise specified. Organolithium reagents were kindly provided by Albemarle Corporation. Solutions were evaporated under reduced pressure with a rotary evaporator. Thin layer chromatography was carried out on aluminum sheets precoated with silica gel 60F254 (Macherey-Nagel, Merck); the spots were visualized under UV light (λ = 254 nm) and/or $KMnO_4$ (aq.) was used as a revealing system. Neutral Aluminum Oxide–Brockmann grade 2 (Alox-BG2) for chromatographic purifications was prepared as we previously reported.[43] MeLi-LiBr (1.5 M ethereal solution) was titrated immediately before use, according to the literature.[44]

The InChI codes of compounds **8–19**, together with some biological activity data, are provided as Supporting Information.

4.1.2 | General procedure for the synthesis of trifluoroacetimidoyl chlorides[45]

To a solution of Ph_3P (3.0 equiv) in 1,2-dichloroethane, CCl_4 (4.0 equiv), Et_3N (1.2 equiv), and trifluoroacetic acid (1.0 equiv) were added at 0°C, and the mixture was stirred for 10 min. After the solution was allowed to reach room temperature, suitable aniline (1.0 equiv) was added. The mixture was then refluxed overnight. The solvent was removed under reduced pressure, and the residue was diluted and washed with *n*-hexane several times and filtered. The filtrate was concentrated under reduced pressure, and the so-obtained crude mixture was subjected to chromatography (silica gel) to afford pure compounds. Spectral information is reported here: 10.1002/ange.201812525.

4.1.3 | General procedure for the synthesis of CMTMAs[32]

To a cooled (−78°C) solution of trifluoromethylchloroimidate (1.0 equiv) in dry THF, chloroiodomethane was added (1.3 equiv). After 2 min, an ethereal solution of MeLi-LiBr (1.2 equiv, 1.5 M) was added dropwise using a syringe pump (flow: 0.200 mL/min). The resulting solution was stirred for 1 h. Then 10% aq solution $NaHCO_3$ (2 mL/mmol substrate) was added, and the reaction mixture was extracted with Et_2O (2 × 5 mL) and washed with water (5 mL) and brine (10 mL). The organic phase was dried over anhydrous Na_2SO_4, filtered, and, after removal of the solvent under reduced pressure, the so-obtained crude mixture was subjected to chromatography (Alox-BG2) to afford pure compounds. Spectral information is reported here: 10.1002/ange.201812525.

4.2 | Pharmacological/biological assays

4.2.1 | Inhibition assay for the chymotrypsin-like activity of the 20S proteasome

The inhibitory activity of the compounds was evaluated by a standard fluorometric method.[36] Human 20S proteasome, isolated and purified from erythrocytes, was obtained from a commercial source (Biomol GmbH), as well as the peptidic substrate (Bachem) Suc-Leu-Leu-Val-Tyr-AMC·HCl for the chymotrypsin-like (ChT-L) activity of the enzyme. The proteolytic activity of the 20S proteasome was measured by monitoring the hydrolysis of the substrate by detecting the fluorescence of the product released, 7-amino-4-methyl coumarin (7-AMC), by means of an Infinite 200 PRO microplate reader (Tecan) at 30°C with a 380 nm excitation filter and a 460 nm emission filter. Human 20S proteasome was employed for testing at a final concentration of 0.004 mg·mL^{-1} together with the fluorogenic substrate (100 μM) and compounds present at 20 μM (screening assay) or at variable concentrations (continuous assay). DMSO was used as a negative control. The reaction buffer consisted of 50 mM Tris pH 7.5, 10 mM NaCl, 25 mM KCl, 1 mM $MgCl_2{\cdot}6H_2O$, 0.03% Sodium dodecyl sulfate (SDS), and 5% DMSO. The compounds and enzyme were incubated for 30 min at 30°C before substrate addition. Product release from substrate hydrolysis was monitored continuously for 10 min. The IC_{50} values were evaluated with the program GraFit® using the two-parameter equation.

4.2.2 | Inhibition assay for the postglutamyl peptide hydrolyzing (PGPH or caspase-like) activity of the 20S proteasome

The assay against the caspase-like (Casp-L) activity of the human 20S proteasome was performed in the same experimental conditions as for the ChT-L activity. The enzyme employed for testing was incubated at a final concentration of 0.003 mg·mL^{-1} together with the appropriate fluorogenic substrate Z-Leu-Leu-Glu-AMC·HCl (80 μM; from Bachem) and compounds present at 20 μM (screening assay). DMSO was used as a negative control. The reaction buffer consisted of 50 mM Tris pH 7.5, 10 mM NaCl, 25 mM KCl, 1 mM $MgCl_2{\cdot}6H_2O$, 0.03% SDS, and 5% DMSO.

4.2.3 | Inhibition assay for trypsin-like activity of the 20S proteasome

The assay against the trypsin-like (T-L) activity of the human 20S proteasome was performed in the same experimental conditions as for the ChT-L and Casp-L activity. The enzyme employed for testing was incubated at a final concentration of 0.0025 mg·mL^{-1} together with the appropriate fluorogenic substrate Boc-Leu-Arg-Arg-AMC·HCl (85 μM; from Bachem) and compounds present at 20 μM (screening assay). DMSO was used as a negative control. The reaction buffer consisted of 50 mM Tris pH 7.4, 50 mM NaCl, 0.5 mM EDTA, 0.03% SDS, and 5% DMSO.

4.2.4 | Inhibition assay for bovine pancreatic α-chymotrypsin

The enzyme (250 μg mL^{-1}) was incubated at 20°C with test compounds (20 μM; screening assay). The reaction buffer consisted

of 50 mM Tris buffer pH 8.0 containing 100 mM NaCl, 5 mM EDTA, and 7.5% DMSO. Product release from fluorogenic substrate hydrolysis (75 µM final concentration, Suc-Leu-Leu-Val-Tyr-AMC; from Bachem) was determined over 10 min.

4.2.5 | Inhibition assay for human cathepsins B and L

Cathepsins B (recombinant, human liver) and L (*Paramecium tetraurelia*) were purchased from Calbiochem. Screening assays with cathepsin B (58 pg mL^{-1}) and cathepsin L (53 ng mL^{-1}) were performed at 20°C with test compounds. Cbz-Phe-Arg-AMC (from Bachem) was used as a fluorogenic substrate for both enzymes (80 µM for cathepsin B, 5 µM for cathepsin L). The reaction buffer consisted of 20 mM Tris buffer pH 6.0 containing 200 mM NaCl, 5 mM EDTA, 2.5 mM dithiothreitol, 0.005% Brij 35, and 10% DMSO. Product release from fluorogenic substrate hydrolysis was determined over 10 min.

4.3 | Molecular docking and dynamics

The studied molecules were drawn using Marvin Sketch and minimized toward molecular mechanics by Merck molecular force field (MMFF94) optimization using the Marvin Sketch geometrical descriptors plugin. The protonation states of the molecules were calculated assuming a 7.4 pH.[46] The MMFF91 obtained 3D structures were subsequently optimized using the parameterized model number six semi-empirical Hamiltonian with the corrections to hydrogen bonding and dispersion (PM6-D3H4) implemented in the MOPAC package (vMOPAC2016). Docking calculations were made using AutoDock Vina, as implemented in the YASARA package, with the default docking parameters. The X-ray crystal structures of the co-crystal proteasome subunit β5/Carmaphycin B (PDB ID: 4HRD) were downloaded from the Protein Data Bank (www.rcsb.org). Only chains K and L were used. Water molecules were also removed. All amino acid residues were kept rigid, whereas all single bonds of ligands were treated as fully flexible for both proteins. A 10 Å simulation cell around all atoms of the cocrystallized ligand was used. AMBER 14 force field was used for the simulation.[29] The MD simulations of the complexes were performed with the YASARA structure package according to our previously reported procedures.[46,47]

ACKNOWLEDGMENTS

The authors thank the University of Vienna, the University of Torino, and the University of Mainz for financial support. All4Labels Group (Hamburg, Germany) is acknowledged for generous funding. The authors acknowledge support from Project CH4.0 under MUR (Italian Ministry for the University) program "Dipartimenti di Eccellenza 2023-2027" (CUP: D13C22003520001).

CONFLICTS OF INTEREST STATEMENT

The authors declare no conflicts of interest.

ORCID

Laura Ielo http://orcid.org/0000-0001-9976-0170

Vittorio Pace http://orcid.org/0000-0003-3037-5930

REFERENCES

[1] A. Hershko, A. Ciechanover, *Annu. Rev. Biochem.* **1998**, *67*, 425.
[2] A. F. Kisselev, A. L. Goldberg, *Chem. Biol.* **2001**, *8*, 739.
[3] K. P. Bhat, S. F. Greer, *Biochim. Biophys. Acta Gene Regul. Mech.* **2011**, *1809*, 150.
[4] K. L. Rock, C. Gramm, L. Rothstein, K. Clark, R. Stein, L. Dick, D. Hwang, A. L. Goldberg, *Cell* **1994**, *78*, 761.
[5] M. H. Glickman, A. Ciechanover, *Physiol. Rev.* **2002**, *82*, 373.
[6] G. N. DeMartino, T. G. Gillette, *Cell* **2007**, *129*, 659.
[7] M. Unno, T. Mizushima, Y. Morimoto, Y. Tomisugi, K. Tanaka, N. Yasuoka, T. Tsukihara, *Structure* **2002**, *10*, 609.
[8] A. F. Kisselev, A. Callard, A. L. Goldberg, *J. Biol. Chem.* **2006**, *281*, 8582.
[9] A. L. Goldberg, *J. Cell Biol.* **2012**, *199*, 583.
[10] H. M. Kim, Y. Yu, Y. Cheng, *Biochim. Biophys. Acta Gene Regul. Mech.* **2011**, *1809*, 67.
[11] A. F. Kisselev, W. A. van der Linden, H. S. Overkleeft, *Chem. Biol.* **2012**, *19*, 99.
[12] M. Groll, L. Ditzel, J. Löwe, D. Stock, M. Bochtler, H. D. Bartunik, R. Huber, *Nature* **1997**, *386*, 463.
[13] A. M. Weissman, N. Shabek, A. Ciechanover, *Nat. Rev. Mol. Cell Biol.* **2011**, *12*, 605.
[14] Y. Cao, Y. Tu, L. Fu, Q. Yu, L. Gao, M. Zhang, L. Zeng, C. Zhang, J. Shao, H. Zhu, Y. Zhou, J. Li, J. Zhang, *Eur. J. Med. Chem.* **2022**, *233*, 114211.
[15] H. Fan, N. G. Angelo, J. D. Warren, C. F. Nathan, G. Lin, *ACS Med. Chem. Lett.* **2014**, *5*, 405.
[16] M. B. Winter, F. La Greca, S. Arastu-Kapur, F. Caiazza, P. Cimermancic, T. J. Buchholz, J. L. Anderl, M. Ravalin, M. F. Bohn, A. Sali, A. J. O'Donoghue, C. S. Craik, *eLife* **2017**, *6*, e27364.
[17] R. Ettari, M. Zappalà, S. Grasso, C. Musolino, V. Innao, A. Allegra, *Pharmacol. Ther.* **2018**, *182*, 176.
[18] L. Kollár, M. Gobec, B. Szilágyi, M. Proj, D. Knez, P. Ábrányi-Balogh, L. Petri, T. Imre, D. Bajusz, G. G. Ferenczy, S. Gobec, G. M. Keserű, I. Sosič, *Eur. J. Med. Chem.* **2021**, *219*, 113455.
[19] K. Takada, F. Van Laethem, Y. Xing, K. Akane, H. Suzuki, S. Murata, K. Tanaka, S. C. Jameson, A. Singer, Y. Takahama, *Nat. Immunol.* **2015**, *16*, 1069.
[20] N. Micale, K. Scarbaci, V. Troiano, R. Ettari, S. Grasso, M. Zappalà, *Med. Res. Rev.* **2014**, *34*, 1001.
[21] Q. Ping Dou, J. A Zonder, *Curr. Cancer Drug. Targets* **2014**, *14*, 517.
[22] D. Chen, M. Frezza, S. Schmitt, J. Kanwar, Q. P. Dou, *Curr. Cancer Drug. Targets* **2011**, *11*, 239.
[23] J. E. Park, Z. Miller, Y. Jun, W. Lee, K. B. Kim, *Transl. Res.* **2018**, *198*, 1.
[24] C. Leonardo-Sousa, A. N. Carvalho, R. A. Guedes, P. M. P. Fernandes, N. Aniceto, J. A. R. Salvador, M. J. Gama, R. C. Guedes, *Molecules* **2022**, *27*, 2201.
[25] G. S. Kaplan, C. C. Torcun, T. Grune, N. K. Ozer, B. Karademir, *Free Radic. Biol. Med.* **2017**, *103*, 1.
[26] D. Schlafer, K. S. Shah, E. H. Panjic, S. Lonial, *Expert Opin. Drug Saf.* **2017**, *16*, 167.
[27] H. Wang, F. Guan, D. Chen, Q. P. Dou, H. Yang, *Expert Opin. Drug Saf.* **2014**, *13*, 1043.

[28] K. Scarbaci, V. Troiano, N. Micale, R. Ettari, L. Tamborini, C. Di Giovanni, C. Cerchia, S. Grasso, E. Novellino, T. Schirmeister, A. Lavecchia, M. Zappalà, *Eur. J. Med. Chem.* **2014**, *76*, 1.
[29] L. Ielo, V. Patamia, A. Citarella, T. Efferth, N. Shahhamzehei, T. Schirmeister, C. Stagno, T. Langer, A. Rescifina, N. Micale, V. Pace, *Int. J. Mol. Sci.* **2022**, *23*, 12363.
[30] M. Groll, N. Gallastegui, X. Maréchal, V. Le Ravalec, N. Basse, N. Richy, E. Genin, R. Huber, L. Moroder, J. Vidal, M. Reboud-Ravaux, *ChemMedChem* **2010**, *5*, 1701.
[31] E. Génin, M. Reboud-Ravaux, J. Vidal, *Curr. Top. Med. Chem.* **2010**, *10*, 232.
[32] (a) L. Ielo, S. Touqeer, A. Roller, T. Langer, W. Holzer, V. Pace, *Angew. Chem.* **2019**, *131*, 2501; (b) L. Ielo, L. Castoldi, S. Touqeer, J. Lombino, A. Roller, C. Prandi, W. Holzer, V. Pace, *Angew. Chem. Int. Ed.* **2020**, *59*, 20852; (c) L. Castoldi, S. Monticelli, R. Senatore, L. Ielo, V. Pace, *Chem. Commun.* **2018**, *54*, 6692.
[33] L. Ielo, V. Pillari, M. Miele, D. Castiglione, V. Pace, *Synlett* **2021**, *32*, 551.
[34] L. Castoldi, S. Monticelli, R. Senatore, L. Ielo, V. Pace, *Chem. Commun.* **2018**, *54*, 6692.
[35] R. L. Stein, F. Melandri, L. Dick, *Biochemistry* **1996**, *35*, 3899.
[36] A. F. Kisselev, A. L. Goldberg, *Methods Enzymol.* **2005**, *398*, 364.
[37] C. A. Lipinski, F. Lombardo, B. W. Dominy, P. J. Feeney, *Adv. Drug Deliv. Rev.* **1997**, *23*, 3.
[38] M. B. Smith, *J. March. [Advanced Organic Chemistry]; March's Advanced Organic Chemistry: Reactions, Mechanisms, and Structure*: Wiley & Sons, New York (USA); **2001**.
[39] D. F. Veber, S. R. Johnson, H.-Y. Cheng, B. R. Smith, K. W. Ward, K. D. Kopple, *J. Med. Chem.* **2002**, *45*, 2615.
[40] B. G. Tabachnick, L. S. Fidell, J. B. Ullman. *Using Multivariate Statistics Vol 6*: Pearson, Boston, MA; **2013**.
[41] M. V. Adv Drug Deliv RevBerridge, A. S. Tan, *Arch. Biochem. Biophys.* **1993**, *303*, 474.
[42] A. Daina, V. Zoete, *ChemMedChem* **2016**, *11*, 1117.
[43] L. Castoldi, W. Holzer, T. Langer, V. Pace, *Chem. Commun.* **2017**, *53*, 9498.
[44] J. Suffert, *J. Org. Chem.* **1989**, *54*, 509.
[45] K. Uneyama, H. Amii, T. Katagiri, T. Kobayashi, T. Hosokawa, *J. Fluorine Chem.* **2005**, *126*, 165.
[46] V. Patamia, G. Floresta, C. Zagni, V. Pistarà, F. Punzo, A. Rescifina, *Int. J. Mol. Sci.* **2023**, *24*, 1425.
[47] D. Gentile, A. Coco, V. Patamia, C. Zagni, G. Floresta, A. Rescifina, *Int. J. Mol. Sci.* **2022**, *23*, 10067.

SUPPORTING INFORMATION

Additional supporting information can be found online in the Supporting Information section at the end of this article.

How to cite this article: L. Ielo, V. Patamia, A. Citarella, T. Schirmeister, C. Stagno, A. Rescifina, N. Micale, V. Pace, *Arch. Pharm.* **2023**;356:e2300174.
https://doi.org/10.1002/ardp.202300174